Eco-friendly Synthesis of benzyl 4-(((4-bromophenyl) sulfonamido)methyl)cyclohexane-1-carboxylate; Physical and Biological Evaluation

Asam Raza, Muhammad*[+]; Danish, Muhammad; Allah Ditta, Mariyam
Department of Chemistry, Hafiz Hayat Campus, University of Gujrat, Gujrat, PAKISTAN

Ur-Rehman, Shafiq
Department of Chemistry, University of Central Punjab, Lahore Campus, Lahore, PAKISTAN

Perveen Malik, Fouzia
Research Center for Modelling and Simulations, National University of Sciences and Technology, H-12 Islamabad, PAKISTAN

Maurin, Jan K.[•]; Budzianowski, Armand
National Centre for Nuclear Research, Andrzeja Sołtana 7, 05-400 Otwock, POLAND

ABSTRACT: *Hydrotreating of heavy naphtha using highly active NiMo catalysts on Walnut shell Activated Carbon (NiMo-WAC) nanocatalysts is a new technology for clean fuel production. In this research, pyrolysis of the walnut shell as a scalable, low-cost, and high-yield method was used to synthesize chemically activated carbon in the presence of $ZnCl_2$, as activating agent. To enhance the catalytic conversion, walnut shell active carbon was functionalized with HCL, HNO_3, and H_2SO_4 to prepare NiMo-WAC1, NiMo-WAC2, and NiMo-WAC3 respectively. These nanocatalysts were synthesized through the incipient wetness impregnation method and characterized by X-Ray Diffraction (XRD), Fourier Transform InfraRed (FT-IR) spectroscopy, inductively coupled plasma-atomic emission spectroscopy (ICP), Field Emission Scanning Electron Microscope (FESEM), Brunauer–Emmett–Reduction (TPR) techniques. CHNS (Eager 300 for EA1112) was used to study elemental analysis of the walnut shell feedstock used for active carbon synthesis. Different operating parameters including temperature, pressure, LHSV, and H_2/feed (heavy naphtha) ratio for hydrodesulfurization (HDS) reaction were explored by evaluating NiMo-WAC nanocatalysts catalytic activity. HDS of heavy naphtha with 2491 ppm of sulfur in the operation condition of temperature: 290 °C, pressure: 30 bar, H_2/oil: 100 NL/L, and LHSV: 3.3 h^{-1} showed considerably higher activity of NiMo-WAC2 nanocatalyst, less than 10 ppm in the product, than NiMo-γAl_2O_3 as a commercial and reference catalyst, maximum 104 ppm in the product, and this is economically valuable.*

KEYWORDS: *Hydrotreating; Walnut shell activated carbon; Nanocatalyst, Heavy naphtha; HDS; NiMo catalysts.*

***** *To whom correspondence should be addressed.*
+ *E-mail: asamgcu@yahoo.com*
• *Other Address: National Medicines Institute, Chełmska 30/34, 00-725 Warsaw, Poland*
1021-9986/2023/1/51-63 13/$/6.03

INTRODUCTION

In the recent years, majority of pharmaceutical companies have decided to decrease their Research and Development (R&D) contribution in chemistry considering synthetic chemistry as more sophisticated technology of lesser importance for modifications in the drug discovery [1, 2]. In contrast to this point of view we admit that excellence and modification in the field of synthetic chemistry might be critically more successful in all aspects of drug discovery and development. Furthermore, modern advancements in new synthetic approaches, such as chemoinformatics, biocatalysis, and reaction iniaturization can stimulate the pace and enhance quality of different products in the pharmaceutical research. The appliance of new synthetic processes has rapidly enlarged the realm of susceptible chemical matter to regulate a vast array of biological objects. There is an increasing appreciation that involves the modification in synthetic chemistry that is altering the method of drug discovery [3, 4]. In this case, we determine some of the utmost permissive advancement in synthetic chemistry along with many opportunities that we consider are poised to alter the proceeding of drug discovery and modification in the upcoming years [5].

Sulfonamides; as significant structural scaffold generally not only present in a variety of different secondary metabolites but also present in many synthetic therapeutics [6]. Therefore, researchers all over the world are committed to synthesizing new compounds having sulfonamide moiety since the past few decades [7-10]. In most of the synthetic approach aniline and its many derivatives were used as a source of nitrogen. Sulfonamide functional groups are present in many sulfa drugs that have considerable biological activity revolutionizing the field of medical sciences [11]. An important chemical such as folic acid that can be used for the synthesis of bacterial RNA and DNA is repressed by sulfonamides; insufficiency of tetrahydrofolate causes the decrease in the production of new RNA and DNA which conclusively decayed the bacteria. Normal growth of microorganisms is constrained due to inaccurate attempt by bacteria that convert sulfonamide rather than *p*-aminobenzoic acid used for the manufacturing of folic acid. As a result of such activity, sulfonamides can be used as antibacterial agents across infections and many other diseases [12, 13].

Alzheimer's Disease (AD) is one of a complicated neurodegenerative disarrangement of the Central Nervous System (CNS) of elderly people, it is the most familiar form of dementia [14]; affecting almost 20 million people all over the world [15, 16] and rapid pervasiveness of AD among the elderly people will increase up to 3 times by 2050 [17]. Alzheimer's disease poses economic and social threats to both developed and developing countries all over the world [18]. For medicinal chemists to slow down or disrupt the onset of AD is one of the ultimate challenges. Currently, a cholinergic assumption is exclusive guidance to resolve the destruction of acetylcholine-a critical neurotransmitter that provides benefits in the communication of motor and nerve cells. A decrease in the acetylcholine level destroys the cognitive actions of the human brain. Regardless of having a moderate success percentage in the treatment of AD, these recommended drugs suffer from negative effects such as diarrhea and nausea. Synthesis of advanced sulfonamides has got major consideration of many researchers for their earlier accomplishments in the field of medicinal chemistry and pharmaceutical sciences. The present study was designed to convert the free acid group of sulfonamide into ester and evaluate its biological activity.

EXPERIMENTAL SECTION

Chemicals Used

The chemicals like ethanol, methanol, dimethyl formamide (DMF), dimethyl sulfoxide (DMSO), benzyl chloride and ethyl acetate were purchased from E. Merck. They were of analytical grade and were used without further purification. UV/Vis spectrophotometer (UV-2300) of Shimadzu while FT-IR of Perkin-Elmer was used for biological studies and characterization of the synthesized compounds respectively.

Synthesis of benzyl 4-(((4-bromophenyl)sulfonamido) methyl)cyclohexane-1-carboxylate [19]

The 4-(((4-bromophenyl)sulfonamido)methyl) cyclohexane-1-carboxylic acid (0.5 g; 1.5 mM) was dissolved in dimethyl formamide (10 mL) with stirring and 15 mL aqueous sodium hydroxide (8 mM) was slowly added to make the solution alkaline. After two hours of stirring at room temperature, benzyl chloride (87 µL) was added drop wise. The reaction was monitored with TLC and after expected completion of the reaction, the flask was kept in the ice bath, resulting in formation of

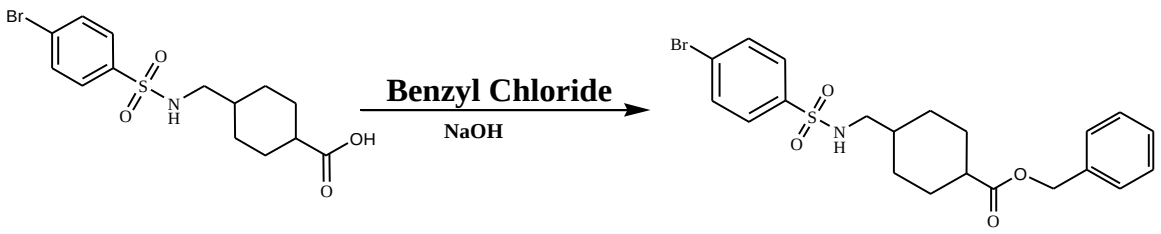

Synthetic Scheme of benzyl 4-(((4-bromophenyl)sulfonamido)methyl)cyclohexane-1-carboxylate

precipitates. The precipitate was filtered, washed with distilled water and re-crystallized in ethyl acetate and *n*-hexane mixture.

Enzyme Inhibition Activity

The inhibition action of AChE (Acetylcholine esterase) and BChE (Butyrylcholine esterase) was tested by the procedures of *Abbasi et al.,* (2012) [20]. The substrates used for AChE and BChE were AChI/BChI respectively. The sample solution (100 µL) having concentration 5 mg/mL, 100 µL enzyme solution and 0.5 mL phosphate buffer (100 mM) of pH 7.8 were used to make the reaction mixture. The mixture was mixed well and kept for 15 minutes. Then 100 µL of substrate (0.5 mM) and 50 µL DTNB (0.2 mM) solution was added and the mixture was incubated at 37°C for almost 20 minutes. Inhibitory activity was calculated using the formula given below and the absorbance was checked at 412 nm:

$$\text{Inhibition}(\%) = \frac{\text{E} - \text{S}}{\text{E}} \times 100 \qquad (1)$$

Where: E = Blank solution absorbance, S = Test sample absorbance

Antibacterial Activity

Shahid *et al.,* (2009) standard protocol was used to measure the antibacterial potential applying the disc diffusion method [21]. Six different bacteria were used to test compounds. Nutrient broth and agar-agar was completely mixed in distilled water to prepare the bacterial medium (10^8 cfu/mL). The uncontaminated medium was loaded in all petri dishes and clotted with bacterial strains one by one. The test samples (20 µL) was applied on discs. Inhibition zone was calculated after 24 hours of incubation at 37°C.

Docking Studies

Docking experiments were performed *via* Molecular Operating Environment (MOE) docking program version 2016.08. Crystal structures of AChE and BChE with PDB codes 1EVE and 1P0I and 4BDS respectively were selected for these studies [22, 23]. The 3D protonation of the downloaded enzymes were done and energy minimization of the retrieved protein molecule was carried out using default parameters of MOE energy minimization algorithm [gradient: 0.05, Force Field: MMFF94X]. The resulting model was subjected to systematic conformational search at default parameters with RMS gradient of 0.01 kcal/mol using Site Finder. Ligand-interaction module of MOE was used to calculate the 2D ligand-enzyme interactions. The view of the docking results and analysis of their surface with graphical representations were done using MOE and discovery studio visualizer [24].

Computational Studies

Geometry optimization was carried out for all synthesized compounds having nitrogen, oxygen and carbon in their structure. Hybrid Becke 3-parameter exchange functional together with the Lee-Yang-Parr correlation functional (B3LYP) was used in density functional theory for calculations. 6-31g basis set was used for C, H, N and oxygen atoms. The DFT calculations were carried out using Gaussian 09 software. The initial geometries were obtained from crystallographic data [25].

Hirshfeld Surfaces Analysis

Hirshfeld surfaces with 2D fingerprint plots were calculated with the help of Crystal Explorer program built in TONTO [26]. A Hirshfeld surface is basically outside curve of the space in which atom or molecule reside in a crystal lattice. The normalized contact distance *d*norm based on both *d*e and *d*i which are calculated from below equation reported by *Aisha et al*., (2020) [27].

$$\text{d}_{\text{norm}} = \frac{(\text{d} - \text{r}_\text{i}\text{vdm})}{\text{r}_\text{i}\text{vdm}} + \frac{(\text{d}_\text{e} - \text{r}_\text{e}\text{vdm})}{\text{r}_\text{e}} \qquad (2)$$

Where *d*e is the distance from the point to the nearest nucleus external to the surface while, *d*i is distance from the point to the nearest nucleus external to the surface.

RESULTS AND DISCUSSION

Single crystal XRD analysis of benzyl 4-(((4-bromophenyl)sulfonamido)methyl) cyclohexane-1-carboxylate

Selected crystal of dimensions ca. 0.8×0.3×0.05 mm, respectively was mounted on an Oxford Xcalibur R diffractometer. After alignment of crystal and the initial diffraction experiment the monoclinic unit cell in the $P2_1/n$ space group was selected. 28488 reflections were collected out of which 4088 were independent. Diffraction data were applied to solve the structure using direct methods from SHELXS-97 [28]. Model of the structure was then refined using SHELXL-97 software [28]. Experimental and refinement parameters are collected in Table 1. The crystal structure of the reactant sulfonamide has been already published by our research group [29], while the structure of synthesized ester was determined via single crystal XRD technique. All non-hydrogen atoms of the title compound were located from E-maps. Consecutive cycles of isotropic and anisotropic refinement enabled localization of all remaining hydrogen atoms from electron difference density maps. In the final cycles of refinement the positional parameters of the non-hydrogen atoms together with their anisotropic displacement parameters were refined as shown in Table 1. Most of hydrogen atoms were included into a model as fixed contributors applying standard geometrical criteria and isotropic displacement parameters tied to respective values of anisotropic parameters for heavy atoms they are bonded to. The final model of the molecule is shown in Figure 1 whereas the crystal packing is shown in Figure 2. Strong N-H···O hydrogen bonds were observe in the structure (shown as the dashed lines in Figure 2). Molecule related by 2_1 screw axes symmetry form hydrogen bonded zigzag chains in the y-direction. The Crystal data of the synthesized ester was deposited at the Cambridge Crystallographic Data Centre, and has been assigned CCDC number 1994386.

Table 1: Crystal data and structure refinement.

Empirical formula	$C_{21}H_{24}BrNO_4S$
Formula weight	466.38
Temperature/K	293(2)
Crystal system	monoclinic
Space group	$P2_1/n$
a/Å	12.75630(10)
b/Å	5.83780(10)
c/Å	28.5390(3)
β/°	96.1150(10)
Volume/Å^3	2113.17(5)
Z	4
ρ_{calc}g/cm^3	1.466
μ/mm^{-1}	3.798
F(000)	960.0
Crystal size/mm^3	0.811 × 0.323 × 0.051
Radiation	Cu Kα (λ = 1.54184 Å)
2Θ range for data collection/°	6.22 to 142.44
Index ranges	-15 ≤ h ≤ 15, -6 ≤ k ≤ 7, -35 ≤ l ≤ 34
Reflections collected	28488
Independent reflections	4088 [R_{int} = 0.0351, R_{sigma} = 0.0225]
Data/restraints/parameters	4088/0/256
Goodness-of-fit on F^2	1.047
Final R indexes [I≥2σ (I)]	R_1 = 0.0365, wR_2 = 0.0979
Final R indexes [all data]	R_1 = 0.0395, wR_2 = 0.1017
Largest diff. peak/hole / e Å^{-3}	0.43/-0.46

Density functional theory

The structure of the targeted compound was confirmed with XRD analysis. In order to compare the theoretical parameters with experimental data (XRD), the obtained structure was optimized with Gaussian software. The bond lengths and bond angels of the understudied molecule was calculated and compared with experimental crystalline output (Table 2 and Table 3). It was observed that there is very good agreement of theoretical and experimental bond lengths and bond angels as shown in Fig. 3 and Fig. 4.

The close agreements of bond angel and bond length contribute the further confirmation of the synthesis of molecule. The maximum bond length deviation was observed in S1-O1 where bond length determined from XRD is 1.4273 Å while DFT is 1.58078 Å, in S1-Oxygen value is 1.58158 Å (DFT) and 1.4367 Å (XRD).

Table 2: Bond Lengths of benzyl 4-(((4-bromophenyl)sulfonamido)methyl)cyclohexane-1-carboxylate.

Atom	Atom	Length/Å		Atom	Atom	Length/Å	
		XRD	DFT			XRD	DFT
Br1	C24	1.8955	1.92026	C4	C10	1.513	1.50444
S1	O1	1.4273	1.58078	C5	C6	1.526	1.53757
S1	O2	1.4367	1.58158	C9	C11	1.498	1.51024
S1	N8	1.5914	1.69517	C11	C12	1.380	1.38877
S1	C21	1.7728	1.79874	C11	C16	1.385	1.38568
O3	C10	1.200	1.20791	C12	C13	1.384	1.38265
O4	C9	1.459	1.46370	C13	C14	1.375	1.38483
O4	C10	1.327	1.35027	C14	C15	1.372	1.38328
N8	C7	1.454	1.48218	C15	C16	1.381	1.38412
C1	C2	1.523	1.54125	C21	C22	1.378	1.37225
C1	C6	1.522	1.53984	C21	C26	1.386	1.37499
C1	C7	1.523	1.53624	C22	C23	1.390	1.38289
C2	C3	1.531	1.53832	C23	C24	1.373	1.37595
C3	C4	1.517	1.53182	C24	C25	1.379	1.38019
C4	C5	1.533	1.54452	C25	C26	1.385	1.37947

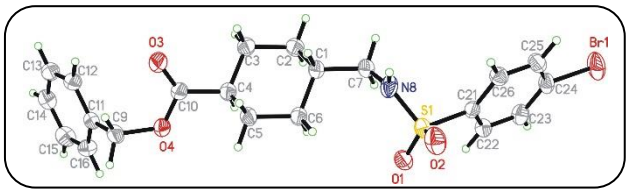

Fig. 1: Conformation of the molecule of the synthesized compound in crystal.

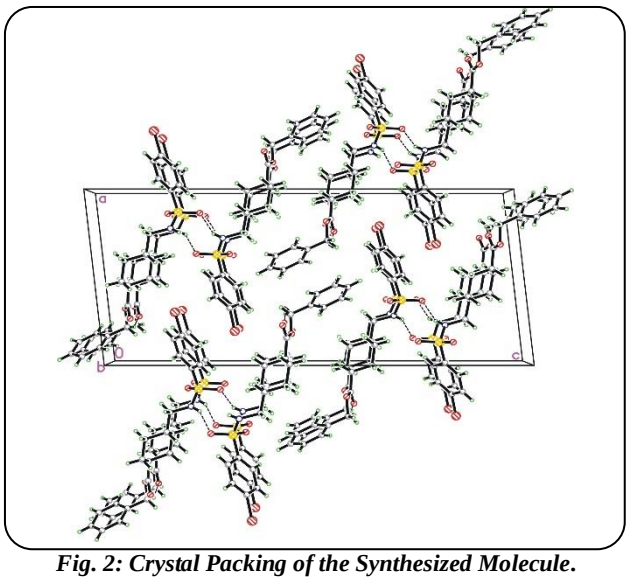

Fig. 2: Crystal Packing of the Synthesized Molecule.

The bond length in S1-N8 is 1.69517 Å and 1.5914 Å calculated from DFT and XRD techniques respectively. Similarly, Oxygen-S1-C21, Oxygen-S1-N8 and N8-S1-C21 bonds showed differences of 6.5827, 7.2441 and 8.030 in bond angels respectively, which may be due to changes in crystalline and gas phases. Normally the theoretical (DFT) calculations belong to gaseous phase while experimentally results (XRD) belong to solid phase, then the calculated optimized structures were compared with their X-ray structures. In the solid state, the differences of bond parameters between the calculated and experimentally may be due to presence of intermolecular interactions which bind the molecules together in crystalline structure [30]. In near past various reports were published about the comparison of theoretical and experimental bond angel and bond length. They have used this tool for the support of the synthetic compounds.

The crystalline molecule was subjected to density functional theory (DFT) and structure was optimized using the basis set cited in the experimental section. The Mulliken charge distribution of the ester was also depicted from the optimized structure using Gaussian software. The oxygen, nitrogen and some carbon atoms have negative charges.

Table 3: Bond Angles of Synthesized Compound.

Atom	Atom	Atom	Angle/°		Atom	Atom	Atom	Angle/°	
			XRD	DFT				XRD	DFT
O1	S1	O2	119.99(11)	117.72374	O3	C10	C4	125.51(18)	126.24306
O1	S1	N8	109.05(9)	105.69038	O4	C10	C4	111.42(16)	111.10133
O1	S1	C21	106.58(8)	113.16267	C12	C11	C9	121.24(19)	120.42749
O2	S1	N8	105.74(11)	112.98410	C12	C11	C16	118.61(18)	119.27485
O2	S1	C21	106.68(9)	105.70726	C16	C11	C9	120.11(19)	120.29490
N8	S1	C21	108.36(9)	100.32980	C11	C12	C13	120.69(19)	120.22789
C10	O4	C9	117.36(16)	119.19179	C14	C13	C12	120.2(2)	120.20241
C7	N8	S1	124.22(14)	120.44564	C15	C14	C13	119.5(2)	119.82147
C2	C1	C6	109.63(16)	109.76216	C14	C15	C16	120.5(2)	119.92738
C7	C1	C2	111.42(16)	109.28354	C15	C16	C11	120.5(2)	120.54424
C7	C1	C6	112.21(15)	111.90570	C22	C21	S1	119.60(14)	117.69440
C1	C2	C3	111.11(16)	111.31296	C22	C21	C26	121.28(16)	121.94088
C4	C3	C2	111.47(16)	110.78192	C26	C21	S1	119.12(13)	120.34574
C3	C4	C5	111.36(16)	110.85350	C21	C22	C23	119.53(17)	118.96888
C10	C4	C3	111.76(16)	110.85350	C24	C23	C22	118.60(18)	119.57222
C10	C4	C5	107.85(15)	110.85350	C23	C24	Br1	118.69(15)	119.61355
C6	C5	C4	111.35(15)	110.85350	C23	C24	C25	122.48(17)	120.97388
C1	C6	C5	111.14(16)	111.12788	C25	C24	Br1	118.83(15)	119.41254
N8	C7	C1	111.56(16)	114.18619	C24	C25	C26	118.77(18)	119.60272
O4	C9	C11	111.46(18)	111.59431	C25	C26	C21	119.33(18)	118.93928
O3	C10	O4	122.98(18)	122.65095					

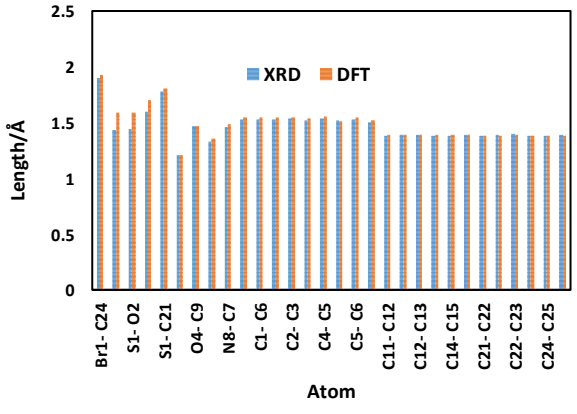

Fig. 3: Comparative bond lengths at SC-XRD and DFT levels for benzyl 4-(((4-bromophenyl)sulfonamido)methyl) cyclohexane-1-carboxylate.

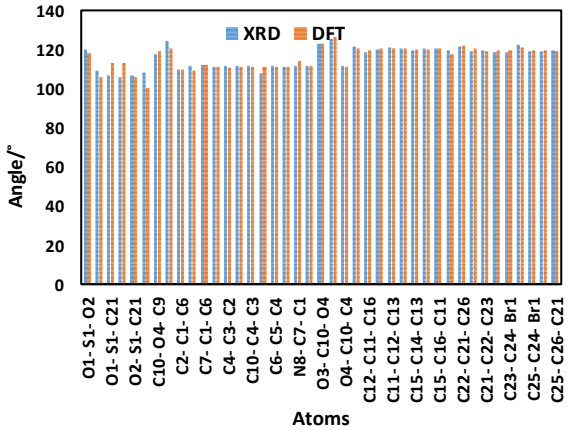

Fig. 4: Comparative of bond angles of SC-XRD and DFT for benzyl 4-(((4-bromophenyl)sulfonamido)methyl)cyclohexane-1-carboxylate.

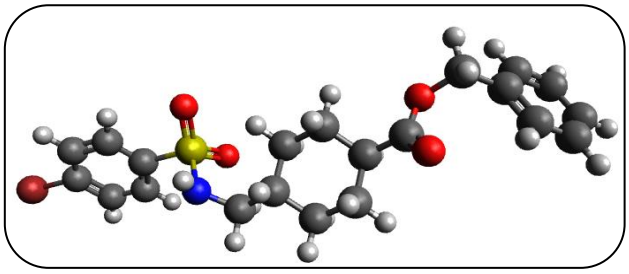

Fig. 5: Optimized Structure of benzyl 4-(((4-bromophenyl)sulfonamido)methyl)cyclohexane-1-carboxylate.

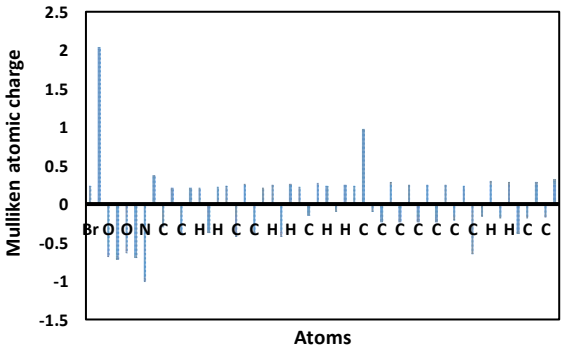

Fig. 6: Mulliken charge distribution of synthesized benzyl 4-(((4-bromophenyl)sulfonamido)methyl)cyclohexane-1-carboxylate.

The sulfur atom has maximum positive charge (2.0261) and nitrogen atom has highest negative charge (-1.0099), while Oxygen has -0.7513 charge. The optimized structure is shown in Fig. 5, while Mulliken charge distribution is shown in Fig. 6.

The various parameters (electronegativity, chemical hardness and chemical potential) were calculated according to Koopmans Theorem [31] (formulae given below) and listed in the Table 4. The energy of HOMO is -0.3375 and that of LUMO is 0.0807, while energy gap (ΔE=(LUMO-HOMO)) between HOMO-LUMO is 0.4183 (hartree) (Figure 7). Electronegativity (x) chemical hardness (η), Ionization Potential (IP), electron affinity (EA) and chemical potential (μ) of synthesized compound has been calculated using the following formulae [32];

$$x = \frac{[E_{LUMO} + E_{HOMO}]}{2} \quad (3)$$

$$\eta = \frac{[E_{LUMO} - E_{HOMO}]}{2} \quad (4)$$

$$\mu = \frac{[E_{HOMO} - E_{LUMO}]}{2} \quad (5)$$

$$IP = -E_{HOMO} \quad (6)$$

$$EA = -E_{LUMO} \quad (7)$$

From optimized structure data we can predict the soft and hard behavior of the molecule on the basis of their energy gaps of HOMO-LUMO. The molecular electrostatic potential (MEP) at various points in the target compound is used to differentiate between positive, negative and neutral charges on the molecule and is depicted with different colors. The order of colors of the molecules is shown according to charge distribution: red > orange > yellow > green > blue [33]. The nitrogen is shown in red and represent region of slight negative potential where electrophilic attack may happen. Hydrogen atoms attached to the ester are shown in blue. DFT also predicted positive potential, which is appropriate site for nucleophilic attack (Figure 8). It is mentioned in many reports that smaller the energy gap between HOMO-LUMO, softener the behavior of the molecule and vice versa [34-36].

Hirshfeld surface analysis

In crystal structure of either organic or inorganic origin, the stability is very important and hydrogen bonding of molecules is a factor, which gives stability in crystal. This hydrogen bonding can be assessed theoretically with Hirshfeld surface analysis. Crystal Explorer is a software applied to determine the Hirshfeld surface of the ester molecule. The surface with a transparent model was shown in three different views (*d*norm, shape index and curvature) in Figure 9. On the surface red, white and blue colors are appearing which depict the strong, intermediate and weak interactions, respectively. In order to explore the hydrogen bonding (interactions) at molecular level, two dimensional finger plots were mapped and individual contribution of each interaction was shown in Fig. 10. It was concluded from 2D plots that major contribution are: H···H (48.3%), O···H (11.5%), H···O (10.1), C···H (8.9%), Br···H (6.4%) and H···C (6.2%) as shown in Fig. 10.

Enzyme Inhibition and Docking Studies

The synthesized molecule was screened against acetylcholine esterase (AChE) and butyrylcholine esterase (BChE) via *in vitro* model according to the reported method. It was found that synthesized compound was

Table 4: Different Parameters Calculated from DFT.

μ (chemical potential)	-0.1284	Ω (electrophilicity index)	0.1284
ŋ (chemical hardness)	-0.2091	IP (ionization potential)	0.33755
X (electronegativity)	0.1284	EA (electron affinity)	-0.08075
HOMO	-0.3375	Dipole moment	2.5730
LUMO	0.0807	Nuclear Repulsion energy	2949.3294
(LUMO-HOMO)	0.4183	Gibbs Free Energy	-4111.7090
Energy (hartree)	-4139.5829	Enthalpy	-4111.6226

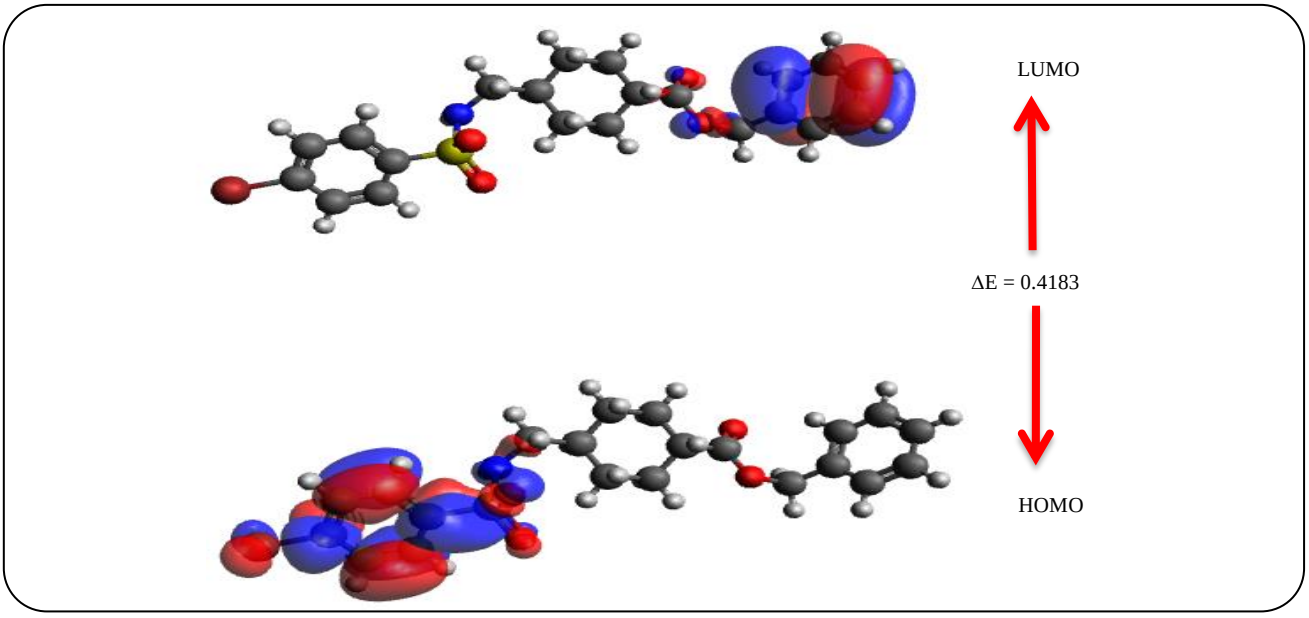

Fig. 7: Energy gap between HOMO and LUMO.

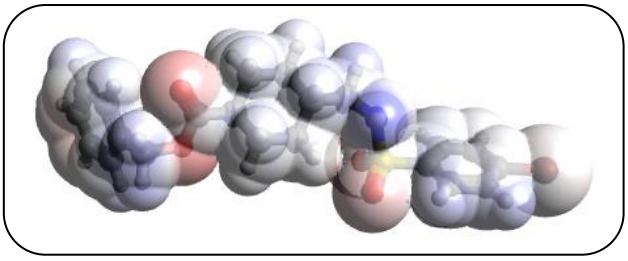

Fig. 8: Molecular Electrostatic Potential.

active against both enzymes. The targeted compound (125 µg) showed 74.5 ± 0.9 % and 56.7 ± 1.1 % inhibition against AChE and BChE, respectively . In order to check the theoretical investigation about enzyme inhibition, docking studies were conducted with esterases by downloading their PDB structures. The details of docking process were explained in the experimental section. The ester was docked with 1EVE (AChE) and 1POI (BChE) as well as 4BDS (BChE). It was observed that understudied compound has shown good docking score as well as binding affinity against all three tested enzyme structures as mentioned in Table 5.

All these outcomes additionally support the experimental observation for the compound that it is a good inhibitor of esterases family and might be used against Alzheimer disease in future after checking other parameters. It was further explained that the compound interacts in the anionic site of the enzymes (AChE and BChE) with hydrogen bonding as well as *pi-pi* interactions. The 2D and 3D interactions of compound with AChE (IEVE) have shown that ester exhibited interaction with Tyr334, Asp72, His440 and Trp84 amino acids located on the active site of the enzyme (Figure 11). Asp72 showed hydrogen bond interactions, while His440 and Trp84 depicted pi-pi interactions. In 1POI (BChE),

Table 5: Docking Score and Binding Affinity of Synthesized Compound.

Compound	Docking Score (Kcal/mol)			Binding Affinity (Kcal/mol)		
	AChE	BChE		AChE	BChE	
	1EVE	1POI	4BDS	1EVE	1POI	4BDS
Ester	-11.7154	-10.1657	-10.5257	-6.9403	-4.5198	-4.0208
Standard	-14.8817	-13.2471	-13.6874	-9.7843	-8.0511	-7.9572

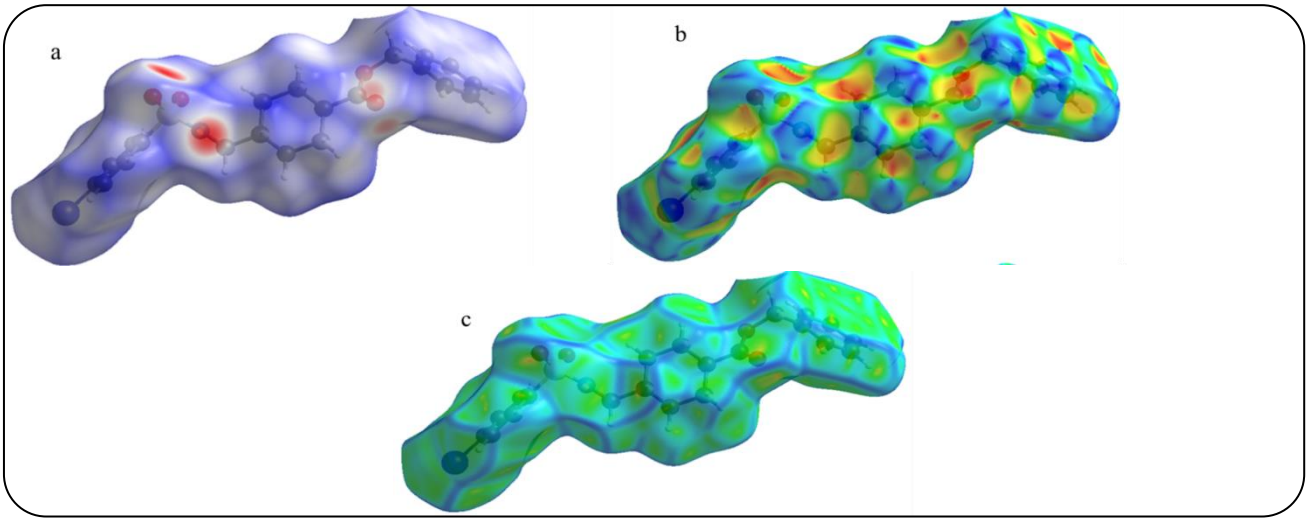

Fig. 9: Hirshfeld surfaces mapped at three views; (a) dnorm, (b) shape index and (c) curvature.

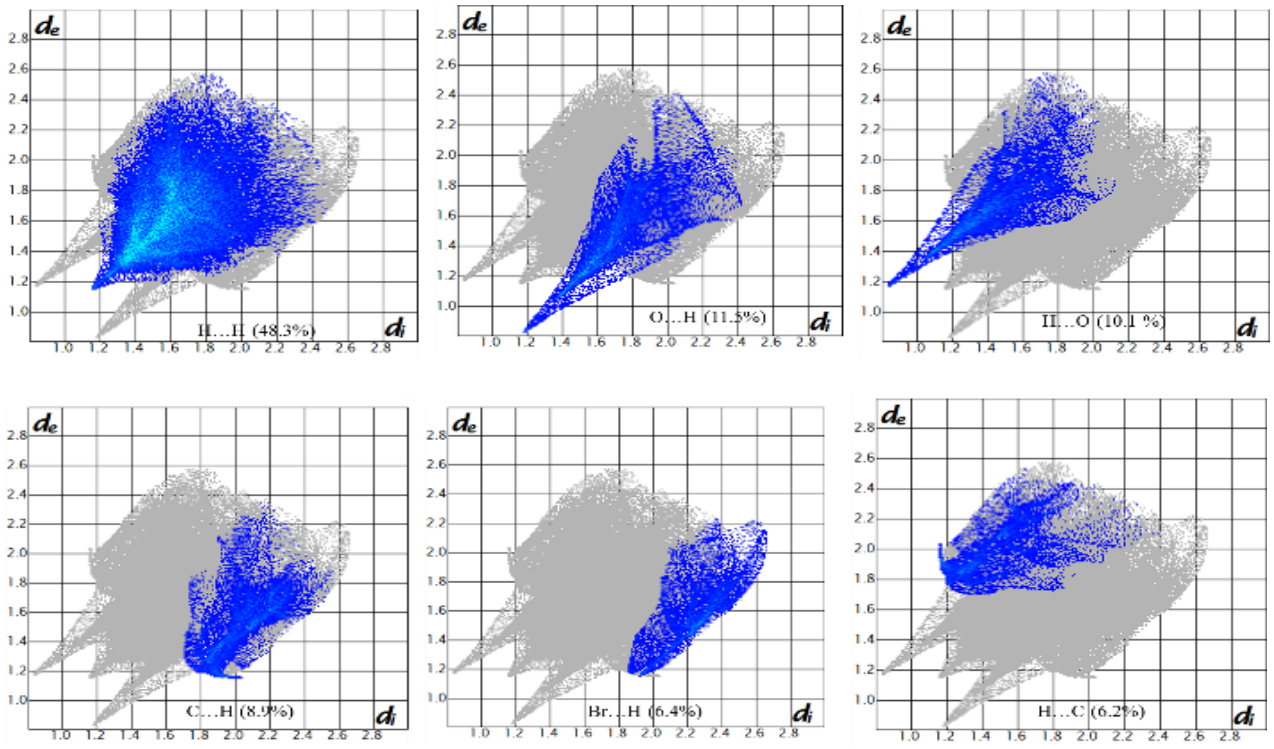

Fig. 10: Fingerprint plot contacts along relative contributions of various intermolecular contacts of benzyl 4-(((4-bromophenyl)sulfonamido)methyl)cyclohexane-1-carboxylate.

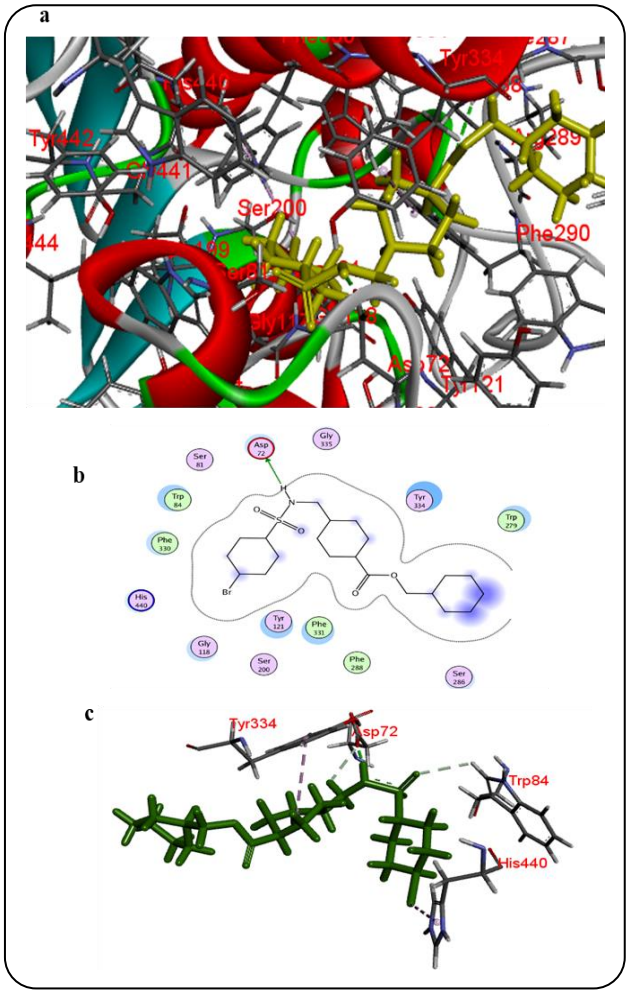

Fig. 11: AChE (IEVE) Interactions of benzyl 4-(((4-bromophenyl)sulfonamido)methyl)cyclohexane-1-carboxylate; (a) close up depiction, (b) 2D interactions and (c) 3D interactions.

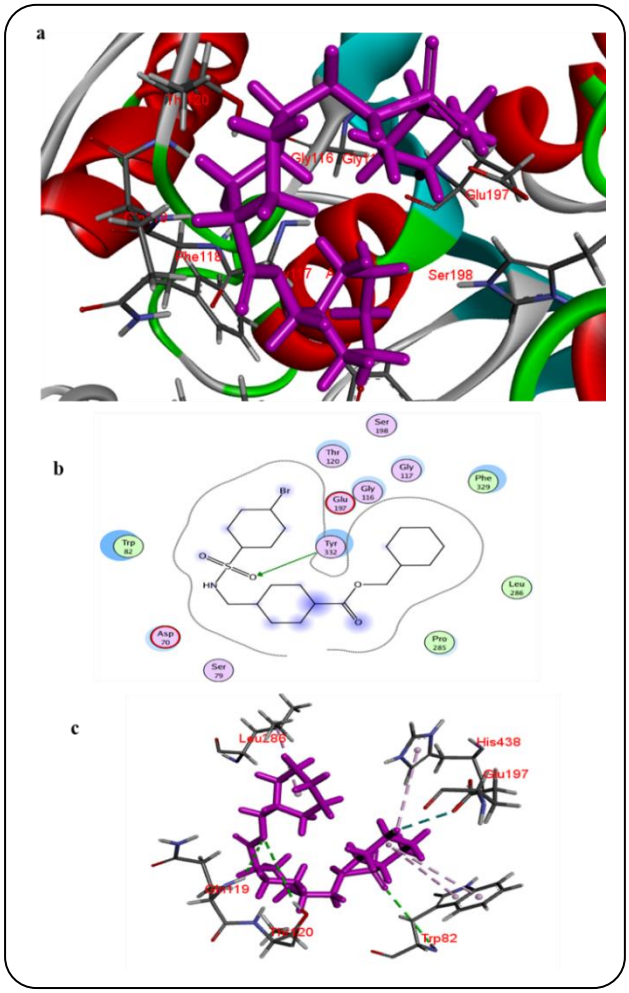

Fig. 12: BChE (1POI) Interactions of benzyl 4-(((4-bromophenyl)sulfonamido)methyl)cyclohexane-1-carboxylate; (a) close up depiction, (b) 2D interactions and (c) 3D interactions.

the compound interacts with Leu286, His438, Glu197, Trp82, Thr120 and Gln119 while in the case of 4BDS (BChE) His438, Trp82, Ala328, Phe329 and Asp70 amino acids have shown interactions with ester (Figure 12 and Figure 13). On 1POI, compound showed hydrogen bond interaction with Thr120, Gln119 and Trp82 while, amino acid residues (His438, Trp82, Leu286 and Glu197) interact through pi-pi interactions. Similarly, the tested compound has interaction with Asp70 (H.B) and with Trp82, His438, Ala328 and Phe329 (π-π).

Antibacterial Potential

The compound was further evaluated in the sense of its antibacterial potential viz agar well diffusion method. The medium was prepared, sterilized and inoculated with respective bacterium in aseptic conditions. The zone of inhibition was measured after 24 hours in mm and it was found that ester has remarkable activity against selected microbes. The activity of the compound was greater (about 30-40%) than streptomycin for most of the microbes except *H. halophila* (Table 6). While in the case of ampicillin its activity is about 50% and comparable o *S. sonnei* (30.1±1.1 mm). All these results give the full support the previous literature, that sulfonamides have good antibacterial activity and are being used in medical field for various ailments or disorders.

CONCLUSIONS

The targeted sulfonamide was synthesized by reported method and its exact structure was elucidated with single

Table 6: Antimicrobial Potential of Synthesized benzyl 4-(((4-bromophenyl)sulfonamido)methyl)cyclohexane-1-carboxylate.

Sample	Zone of inhibition (mm)					
	Bacterial strains					
	C. salixgens[a]	*H. halophila* [b]	*E.coli*[c]	*S. aureus*[d]	*B. subtilis*[e]	*S. sonnei*[f]
Ester	NIL	7.3±0.7	15.4±0.4	12.1±0.9	17.5±1.1	30.1±1.1
Streptomycin	NIL	14.1±1.2	8.9±0.8	8.5±0.8	9.3±0.9	15.3±1.0
Ampicillin	NIL	15.6±0.7	33.5±1.1	39.2±1.0	41.3±1.3	31.5±1.1

a) Chromohalobacter salixgens, b) Halomonas halophila, c) Escherichia coli, d) Staphylococcus aureus, e) Bacillus subtilis, f) Shigella sonnei.

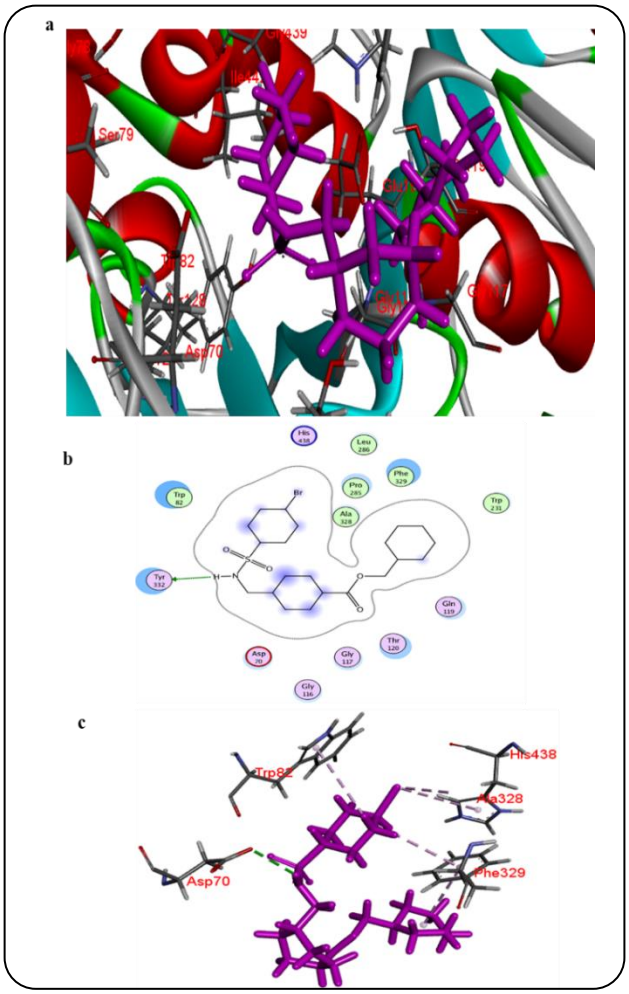

Fig. 13: BChE (4BDS) Interactions of benzyl 4-(((4-bromophenyl)sulfonamido)methyl)cyclohexane-1-carboxylate; (a) close up depiction, (b) 2D interactions and (c) 3D interactions.

X-Ray technique. The structure was optimized through density functional theory using proper basis set. The theoretical and experimental structure parameters were correlated which are in close agreement to each other.

The synthesized compound was further screened against different microbes which depicted that benzyl 4-(((4-bromophenyl)sulfonamido)methyl)cyclohexane-1-carboxylate has ability to retort the growth of different bacterial strains. It was concluded from results that synthesized compound is stable on the basis of its energy gap value and correlation studies in favor for the stability of the compound. Hirshfeld analysis and finger plot interactions also supported the crystalline structure of the ester. Furthermore, antibacterial and enzyme inhibition screening suggested that this molecule has potential to inhibit the esterase enzyme as well as growth of the various microorganism. In order to confirm the *in vitro* application of the compound as enzyme inhibitor, in-silico docking study was done which revealed that synthesized compound has good docking score and may be used as enzyme inhibitor for medicinal application. It is further confirmed that both pdb files of BChE have about same results in the form of docking score and binding energy.

Acknowledgment

The authors are thankful to Higher Education Commission (HEC) of Pakistan for funding this work under the Project No. 20-2549/NRPU/R&D/HEC/12.

Received : Dec. 7, 2021 ; Accepted : Feb. 28, 2022

REFERENCES

[1] Ball P., Chemistry: why Synthesize? *Nature News*, **528(7582)**: 327-329 (2015).

[2] Whitesides G M., Reinventing Chemistry, *Angewandte Chemie International Edition*, **54 (11)**: 3196-3209 (2015).

[3] Blakemore D.C., Castro L., Churcher I., Rees D.C., Thomas A.W., Wilson D.M., Wood A., Organic Synthesis Provides Opportunities to Transform Drug Discovery, *Nature Chemistry*, **10**: 383-394 (2018).

[4] Gerry C.J., Schreiber S.L., Chemical Probes and Drug Leads from Advances in Synthetic Planning and Methodology, *Nature Reviews Drug Discovery*, **17**: 333-352 (2018).

[5] Campos K.R., Coleman P.J., Alvarez, J.C., Dreher S.D., Garbaccio R.M., Terrett N.K., Tillyer R.D., Truppo M.D., Parmee E.R., The Importance of Synthetic Chemistry in the Pharmaceutical Industry, *Science*, **363**: 1-8 (2019).

[6] Feng M., Tang B., Liang S., Jiang X., Sulfur Containing Scaffolds in Drugs: Synthesis and Application In Medicinal Chemistry, *Current Topics in Medicinal Chemistry*, **16**: 1200-1216 (2016).

[7] Hussein E.M., Al-Rooqi M.M., Abd El-Galil S.M., Ahmed S.A., Design, Synthesis, and Biological Evaluation of Novel N 4-substituted Sulfonamides: Acetamides Derivatives as Dihydrofolate Reductase (DHFR) Inhibitors, *BMC Chemistry*, **13(91)**: 1-18 (2019).

[8] Hassan S A., Synthesis, Spectroscopic Study and Biological activity of some New Heterocyclic Compounds Derived from Sulfadiazine, *Zanco Journal of Pure and Applied Sciences*, **31(6):** 92-109 (2019).

[9] Hassan S.A., Aziz D.M., Synthesis, in Vitro Antimicrobial Assay and Molecular Docking Studies of Some New Symmetrical Bis-Schiff Bases and their 2-Azetidinones, *Zanco Journal of Pure and Applied Sciences*, **33(2)**: 34-50. 2021

[10] Hassan S A., Aziz D M., Synthesis of New Series Bis-3-Chloro-β-Lactam Derivatives from Symmetrical Bis-Schiff Bases as Effective Antimicrobial Agents with Molecular Docking Studies, *Science Journal of University of Zakho*, **9**: 128-137 (2021).

[11] Ali A., Reddy G K K., Cao H., Anjum S G., Nalam M N., Schiffer C A., Rana T M., Discovery of HIV-1 Protease Inhibitors with Picomolar Affinities Incorporating N-Aryl-Oxazolidinone-5-Carboxamides as Novel P2 ligands, *Journal of Medicinal Chemistry*, **49**: 7342-7356 (2006)

[12] Li R., Kenyon G.L., Cohen F.E., Chen X., Gong B., Dominguez J.N., Davidson E., Kurzban G., Miller R.E., Nuzum E.O., In Vitro Antimalarial Activity of Chalcones and their Derivatives, *Journal of Medicinal Chemistry*, **38**: 5031-5037 (1995).

[13] Abdel-Wahab B.F., Abdel-Aziz H.A., Ahmed E.M., Synthesis and Antimicrobial Evaluation of Some 1, 3-thiazole, 1, 3, 4-thiadiazole, 1, 2, 4-triazole, and 1, 2, 4-triazolo [3, 4-b][1, 3, 4]-thiadiazine Derivatives Including a 5-(benzofuran-2-yl)-1-phenylpyrazole Moiety, *Monatshefte für Chemie-Chemical Monthly*, **140**: 601-605 (2009).

[14] Pietrzik C., Behl C., Concepts for the Treatment of Alzheimer's Disease: Molecular Mechanisms and Clinical Application, *International Journal of Experimental Pathology*, **86**: 173-185 (2005).

[15] Raymond S.B., Treat L.H., Dewey J.D., McDannol N.J., Hynynen K., Bacskai B.J., Ultrasound Enhanced Delivery of Molecular Imaging and Therapeutic Agents in Alzheimer's Disease Mouse Models, *PloS One*, **3**: e2175 (2008).

[16] Yar M., Arshad M., Farooq A., Gilani M A., Ayub K., Ejaz A., Kumar A., Ninomiya I., Synthesis and DPPH Scavenging Assay of Reserpine Analogues, Computational Studies and in Silico Docking Studies in AChE and BChE Responsible for Alzheimer's Disease, *Brazilian Journal of Pharmaceutical Sciences*, **51**: 53-61 (2015).

[17] Apostolova L.G., Dinov I.D., Dutton R.A., Hayashi K.M., Toga A.W., Cummings J.L., Thompson P.M., 3D Comparison of Hippocampal Atrophy in Amnestic Mild Cognitive Impairment and Alzheimer's Disease, *Brain*, **129**: 2867-2873 (2006).

[18] Wang G., Cheng Q., Zhang S., Bai L., Zeng J., Cui P.J., Zhang T., Sun Z K., Ren R J., Deng Y L., Economic Impact of Dementia in Developing Countries: An Evaluation of Alzheimer-Type Dementia in Shanghai, China, *Journal of Alzheimer's Disease*, **15**: 109-115 (2008).

[19] Gomberg M., Buchler C., The Preparation of Benzyl Esters and other Benzyl-Derivatives from Benzyl Chloride, *Journal of the American Chemical Society*, **42**: 2059-2072 (1920).

[20] Abbasi M., Ilyas M., Sonia A., Shahwar D., Raza M., Khan K., Ashraf M., Afzal I., Ambreen N., Curcumin and its Derivatives: Moderate Inhibitors of Acetylcholinesterase, Butyrylcholinesterase and Trypsin, *Scientia Iranica*, **19**: 1580-1583 (2012).

[21] Shahid S., Raza M A., Ur-Rehman S., Synthesis, Characterization and Antimicrobial Potential of Transition Metal Complexes of Triacetic Lactone, *African Journal of Biotechnology*, **8**: 5116-5121 (2009).

[22] Danish M., Bibi A., Raza M.A., Noreen N., Arshad M.N., Aisri M A., Sulfonamide Derived Esters: Synthesis, Characterization, Density Functional Theory and Biological Evaluation through Experimental and Theoretical Approach, *Acta Chimica Slovenica*, **67**: 785-798 (2020).

[23] Dege N., Raza M.A., Doğan O E., Ağar T., Mumtaz M.W., Theoretical and Experimental Approaches of New Schiff Bases: Efficient Synthesis, X-Ray Structures, DFT, Molecular Modeling and ADMET Studies, *Journal of the Iranian Chemical Society*, **18**: 2345-2368 (2021).

[24] Danish M., Raza M A., Anwar U., Rashid U., Ahmed Z., Differential Functional Theory and Molecular Docking Studies of Newly Synthesized Carbamates, *Journal of the Chinese Chemical Society*, **66(11)**: 1408-1415 (2019).

[25] Danish M., Bibi A., Gilani K., Raza M.A., Ashfaq M., Arshad M.N., Asiri A.M., Ayub K., Antiradical, Antimicrobial and Enzyme Inhibition Evaluation of Sulfonamide Derived Esters, Synthesis, X-Ray Analysis and DFT Studies, *Journal of Molecular Structure*, **1175**: 379-388 (2019).

[26] Wolff S., Grimwood D., McKinnon J., Turner M., Jayatilaka D., Spackman M., "Crystal Explorer" package, ver. 3.1. *University of Western Australia, Perth, Australia* (2013).

[27] Aisha, Raza M A., Sumrra S H., Javed K., Saqib Z., Maurin J K., Budzianowski A., Synthesis, Characterization and Molecular Modeling of Amino Derived Thiazolidinones as Esterase and Glucosidase Inhibitors, *Journal of Molecular Structure*, **1219**: 128609 (2020).

[28] Sheldrick G M., A Short History of SHELX, *Acta Crystallographica Section A*, **64**: 112-122 (2008).

[29] Ashfaq M., Arshad M N., Danish M., Asiri A M., Khatoon S., Mustafa G., Zolotarev P N., Butt R A., Şahin O., Synthesis and Description of Intermolecular Interactions in New Sulfonamide Derivatives of Tranexamic Acid, *Journal of Molecular Structure*, **1103**: 271-280 (2016).

[30] Murugavel S., Vijayakumar S., Nagarajan S., Ponnuswamy A., Crystal Structure and DFT Studies of 4-(1-Benzyl-5-Methyl-1h-1, 2, 3-Triazol-4-Yl)-6-(3-Methoxyphenyl) Pyrimidin-2-Amine, *Journal of the Chilean Chemical Society*, **59**: 2640-2646 (2014).

[31] Dwivedi A., Baboo V., Bajpai A., Fukui Function Analysis and Optical, Electronic, and Vibrational Properties of Tetrahydrofuran and its Derivatives: A Complete Quantum Chemical Study, *Journal of Theoretical Chemistry*, 345234 (2015).

[32] Raza M.A., Fatima K., Molecular Modeling Approach for Designing of Amino-Derived Anti-Alzheimer Agents: A Computational Study, *Journal of Physical Organic Chemistry*, **33**: e4076 (2020).

[33] Sumrra S. H., Kausar S., Raza M A., Zubair M., Zafar M N., Nadeem M A., Mughal E U., Chohan Z H., Mushtaq F., Rashid U., Metal Based Triazole Compounds: Their Synthesis, Computational, Antioxidant, Enzyme Inhibition and Antimicrobial Properties, *Journal of Molecular Structure*, **1168**: 202-211 (2018).

[34] Jensen F., "Introduction to Computational Chemistry". John Wiley & Sons Inc. (2017).

[35] Tang C L., "Fundamentals of Quantum Mechanics: for Solid State Electronics and Optics", Cambridge University Press (2005).

[36] Gotwals R., Sendlinger S., "A Chemistry Educator's Guide to Molecular Modeling". The North Carolina School of Science and Mathematics, Durham, NC (2007).